SLOW EARTHQUAKES

Newsletter04

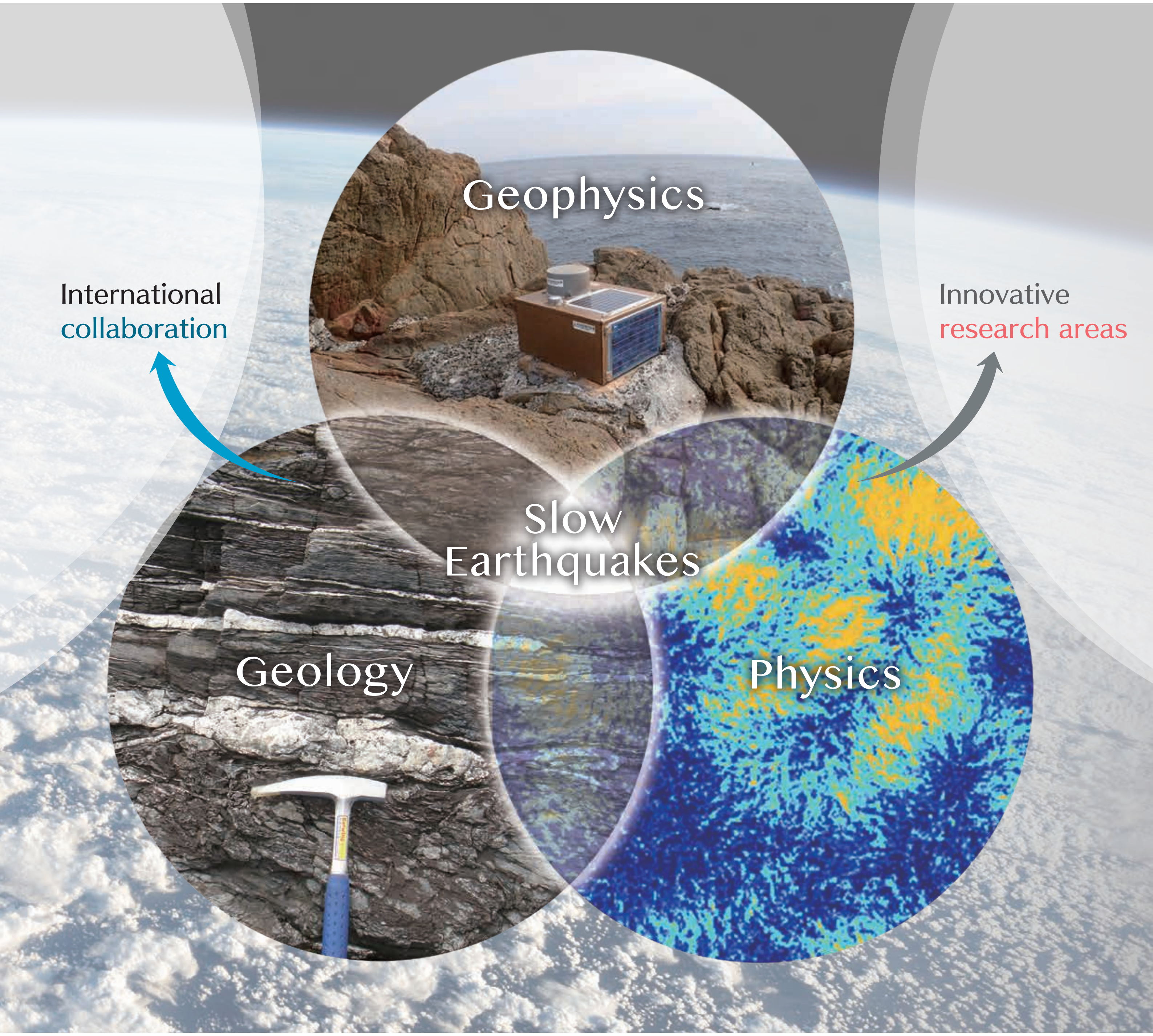

2016–2020 Japan Society for the Promotion of Science
Grant-in-Aid for Scientific Research
on Innovative Areas (JSPS KAKENHI No.2804)

INDEX

Introduction to Research in Group A01

Low-frequency tremor in the Japan Trench subduction zone detected using S-net

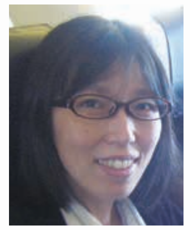

Sachiko TANAKA, Network Center for Earthquake, Tsunami and Volcano, National Research Institute for Earth Science and Disaster Resilience

Low-frequency tremor, with a dominant frequency of several hertz, was first discovered in the Nankai Trough subduction zone in Southwest Japan (Obara, 2002) using the High Sensitivity Seismograph Network Japan (Hi-net), which was installed by the National Research Institute for Earth Science and Disaster Resilience (NIED) after the 1995 Kobe Earthquake. Tremor has since been widely recognized in many subduction zones, and often occurs on the plate interface, just downdip or updip of megathrust seismogenic zones (e.g., Obara and Kato, 2016). However, it has yet to be directly measured in the Japan Trench subduction zone in Northeast Japan.

NIED installed the world's largest seafloor observation network, the Seafloor Observation Network for Earthquakes and Tsunamis along the Japan Trench (S-net), after the 2011 Tohoku-Oki Earthquake for the rapid detection of offshore earthquakes and tsunamis. This network covers a wide offshore area from Hokkaido to the Boso Peninsula, and includes 150 seismic stations, which consist of seismometers and pressure gauges. The observed data are transmitted onshore in real time via submarine cables. Such seafloor observations also provide invaluable data for extensive research studies on offshore slow earthquakes. We have reported the first observations of tremor off Tokachi and Sanriku in the Japan Trench subduction zone using S-net (Tanaka *et al.*, 2019).

The observed tremor occurs within a narrow zone of the subducting plate interface, between the 10- and 25-km depth contours, and is concentrated in two regions off Tokachi and Sanriku, with these regions separated by a gap (Fig.1a). Very low frequency earthquakes (VLFEs), with a predominant period of 10–100 s, have been identified in the regions off Tokachi and Sanriku using seismic data from onshore networks

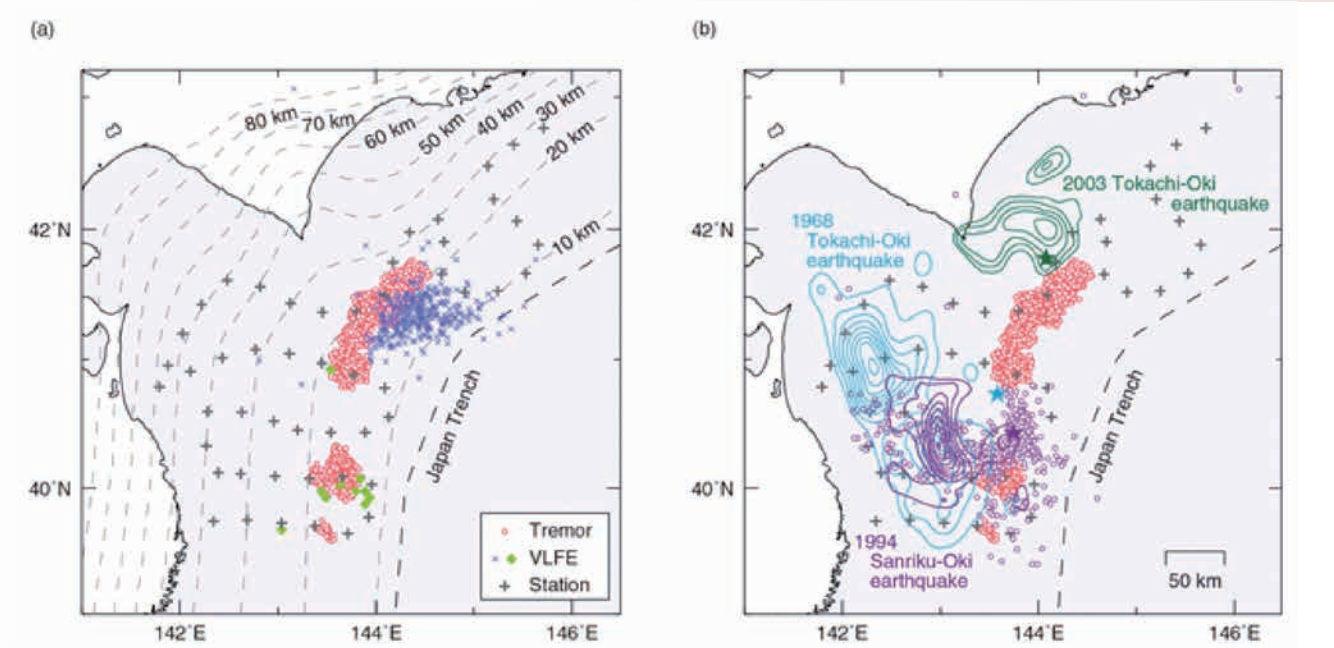

Fig. 1.
Locations of the tremor sources during the January 2017–September 2018 period (red circles). The S-net station locations used in this study are indicated by the black plus symbols. (a) Tremor source locations relative to the very low frequency earthquake (VLFE) locations. The blue crosses (Asano *et al.*, 2008) and green diamonds (Matsuzawa *et al.*, 2015) denote the VLFE locations, which were determined using onshore networks. The broken lines are the depth contours of the plate interface (Kita *et al.*, 2010; Nakajima and Hasegawa, 2006). (b) Tremor source locations relative to the three great earthquakes in the region over the past half century. The contours and stars indicate the slip distributions (Nagai *et al.*, 2001; Yamanaka and Kikuchi, 2003, 2004) and epicenters of the three great earthquakes, respectively. The purple circles denote the aftershock distribution ($M \geq 3.0$) for the seven days following the 1994 Sanriku-Oki Earthquake.

(Asano *et al*., 2008; Matsuzawa *et al*., 2015). The observed tremor occurs at similar locations to those VLFEs.

Three megathrust earthquakes (1968 Tokachi-Oki, 1994 Sanriku-Oki, and 2003 Tokachi-Oki earthquakes) have occurred in this area over the past half-century. The tremor sources are located near the updip edges of the slip areas of these giant earthquakes (Fig.1b). The ruptures of the 1968 Tokachi-Oki and 1994 Sanriku-Oki earthquakes initiated within a gap between the tremor zones off Tokachi and Sanriku, and the aftershocks of the 1994 earthquake were also broadly distributed within this gap, indicating that tremor avoids the epicentral and aftershock areas of these large subduction-zone earthquakes.

This analysis also reveals various tremor characteristics, including their durations and recurrence intervals, both of which vary with location along the trench. The tremor locations and variations in their properties imply lateral heterogeneities in the behavior of plate-boundary slip near the Japan Trench. These observations will provide valuable insights into the frictional properties at the shallow plate interface in this region.

References

Asano, Y., *et al*. (2008), *Earth Planets Space* 60, 871-875, doi:10.1186/BF03352839.

Kita, S., *et al*. (2010), *Earth Planet. Sci. Lett.* 290, 415-426, doi:10.1016/j.epsl.2009.12.038.

Matsuzawa, T., *et al*. (2015), *Geophys. Res. Lett.* 42, 4318-4325, doi:10.1002/2015GL063959.

Nagai, R., *et al*. (2001), *Zishin* 54, 267–280, doi:10.4294/zisin1948.54.2_267.

Nakajima, J., and Hasegawa, A. (2006), *Geophys. Res. Lett.* 33, L16309, doi:10.1029/2006GL026773.

Obara, K. (2002), *Science* 296, 1679-1681, doi:10.1126/science.1070378.

Obara, K., and Kato, A. (2016), *Science* 353, 253-257, doi:10.1126/science.aaf1512.

Tanaka, S., *et al*. (2019), *Geophys. Res. Lett.* 46, 5217-5224, doi:10.1029/2019GL082817.

Yamanaka, Y., and Kikuchi, M. (2003), *Earth Planets Space* 55, e21-e24, doi:10.1186/BF03352479.

Yamanaka, Y., and Kikuchi, M. (2004), *J. Geophys. Res.* 109, B07307, doi:10.1029/2003JB002683.

Introduction to Research in Group A02

Precise gravity observations reveal the crustal fluid behavior during slow slip events

Yoshiyuki TANAKA, Graduate School of Science, The University of Tokyo

The gravitational field of the Earth changes in space and time due to various phenomena (Crossley *et al*., 2013; Wouters *et al*., 2014). A representative phenomenon is the solid Earth tides. Gravity changes during the course of a day amount to 100 µGal, where 1 µGal (10^{-8} ms^{-2}) corresponds to approximately 10^{-9} of the average gravity on the Earth's surface. Recent terrestrial and satellite measurements have detected gravity changes on the order of microGals due to earthquakes and volcanic activity. Here we successfully detected gravity changes of several microGals that were synchronized with the occurrence of long-term slow slip events (SSEs) for the first time (Tanaka *et al*., 2018).

The study area is shown in Fig.1a. The three gravity measurement sites are located at the updip extent of the plate interface (OMZ), center of the slow slip distribution (TYH), and between OMZ and TYH (KKG). An FG5 absolute gravimeter, with an accuracy of 1–2 µGal, is used for the measurements (Fig.2). The trajectory of the free-falling corner cube in the vacuum chamber is precisely determined using a laser interferometer and Rubisium clock. Each observation at a given site consisted of a continuous 2–3-day occupation to effectively remove the tidal effects. The observations are shown in Fig.1b. We have corrected for the Bouguer anomaly due to the crustal vertical motion using Global Navigation Satellite System data. The gravity does not change during the two SSEs, whereas it increases between these two events (Fig.1b).

We interpreted this observed change by assuming that the secular increases at the three sites were caused by factors other than SSEs, and considered a possible mechanism where SSEs would cause a decrease in gravity. Fault slip on the plate interface was estimated to contribute <1 µGal to the gravity change based on the theory of Okubo (1992), such that fault slip could not explain the observations. Kato *et al*. (2010) have indicated fluids in this slow slip area. Therefore, we assumed that such fluids could migrate updip along the plate interface based on fault-valve behavior (Sibson, 1992), whereby slip increases the permeability within the fracture zone. We derived an analytical expression for the fluid pressure by modifying the theory of Dr. Suzuki in the physics group (C02) (Suzuki and Yamashita, 2006), which states that pressure changes cause density changes. We determined the permeability that reproduced the observed gravity changes, and obtained a permeability value of approximately 10^{-15} m^2.

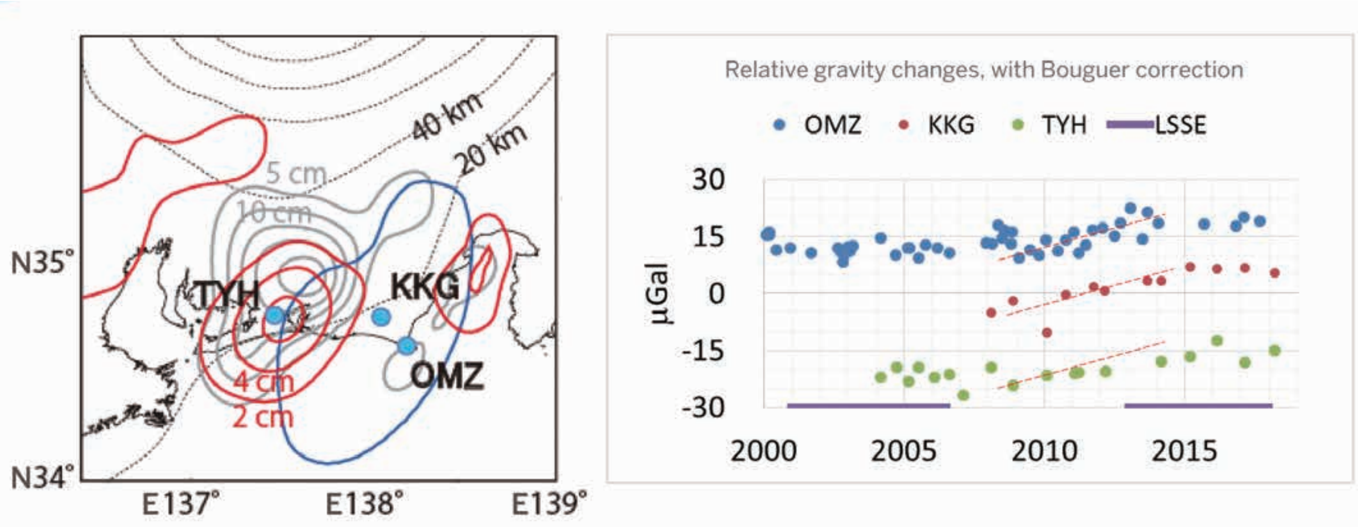

Fig. 1.
(a) Locations of the gravity observation sites. The gray and red contours show the amount of accumulated slow slip during the 2001–2005 and 2013–2017 periods, respectively (Geospatial Information Authority of Japan, 2017). The dotted lines denote the depth contours of the plate interface. (b) Observed gravity changes. The effects of crustal deformation (Bouguer anomaly) have been removed. The error bars are too small to see at this scale. The three dotted red lines were drawn to show that the gravity change occurs at the same rate at each gravity observation site between the two SSEs.

The obtained permeability value is within the range of previously determined values, which are based on laboratory experiments and numerical simulations (e.g., Katayama *et al*., 2012; Yamashita, 2013). The thickness of the fracture zone is proportional to the predicted gravity change in our model. The adopted thickness of 1 km is larger than that inferred from geological observations. We are currently collaborating with the physics group to solve this problem by developing a new model that incorporates crustal deformation outside of the fracture zone. We will then work with the geology group (B02) to evaluate the validity of this model.

We have initiated similar gravity observations in other slow slip areas in Japan. If these continued observations are able to reproduce the gravity changes, then they will provide considerable insight into various earthquake processes, including SSE mechanisms, the earthquake cycle, and water circulation in subduction zones.

Finally, we acknowledge Nagoya University and Shizuoka University for supporting the gravity observations.

Fig. 2.
FG5 absolute gravimeter. We conducted repeated annual campaign measurements because high costs prohibited continuous observations.

References

Crossley, D., *et al*. (2013), *Rep. Prog. Phys.* 76, 046101 (47pp), doi:10.1088/0034-4885/76/4/046101.

Geospatial Information Authority of Japan (2017), *Rep. Coord. Comm. Earthq. Predict*. 98, 197–241.

Katayama, I., Terada, T., Okazaki, K., Tanikawa, W. (2012), *Nat. Geosci*., Episodic tremor and slow slip potentially linked to permeability contrasts at the Moho, 5:731–734. https://doi.org/10.1038/NGEO1559

Kato, A., *et al*. (2010), *Geophys. Res. Lett.* 37, L14310, https://doi.org/10.1029/2010GL043723.

Sibson, R.H. (1992), *Tectonophysics* 211, 283–293.

Suzuki, T., and Yamashita, T. (2006), *J. Geophys. Res.* 111, B03307, https://doi.org/10.1029/2005JB003810.

Tanaka, Y., *et al*. (2018), *Earth Planets Space* 70, 25, https://doi.org/10.1186/s40623-018-0797-5.

Wouters, B., *et al*. (2014), *Rep. Prog. Phys.* 77, 116801 (41pp), http://dx.doi.org/10.1088/0034-4885 /77/11/116801.

Yamashita, T. (2013), *Geophys. J. Int*. 193:375–393. https://doi.org/10.1093/gji/ggs117

Introduction to Research in Group B01

Preliminary results from the Network- and marine-MT surveys in the western margin of the Nankai subduction zone

Makoto UYESHIMA, Earthquake Research Institute, The University of Tokyo

Hiroshi ICHIHARA, Earthquake and Volcano Research Center, Nagoya University

Interstitial fluids are believed to control the occurrence of slow earthquakes. Electrical resistivity is a physical property that is sensitive to interstitial fluids and geology, and can therefore be used to infer the presence of fluids in the system. Here we present preliminary results from the Network- and marine-magnetotelluric (MT) surveys we have been conducting in the western margin of the Nankai subduction zone to clarify the spatial distribution and temporal variations in resistivity.

Network-MT survey

Network-MT surveys enable the acquisition of undistorted electrical potential data using a metallic telephone line network. We measured the electrical potential difference with long baselines in 17 areas using the Nippon Telegraph and Telephone Corp. network (**red lines in Figs.1 and 2a**). We also measured the geomagnetic field at two stations in the target region (**red circles in Fig.1**). The high-quality frequency-domain response functions between the electric and magnetic fields were estimated. We obtained the resistivity structure in the target region after a three-dimensional (3-D) inversion of the estimated fields.

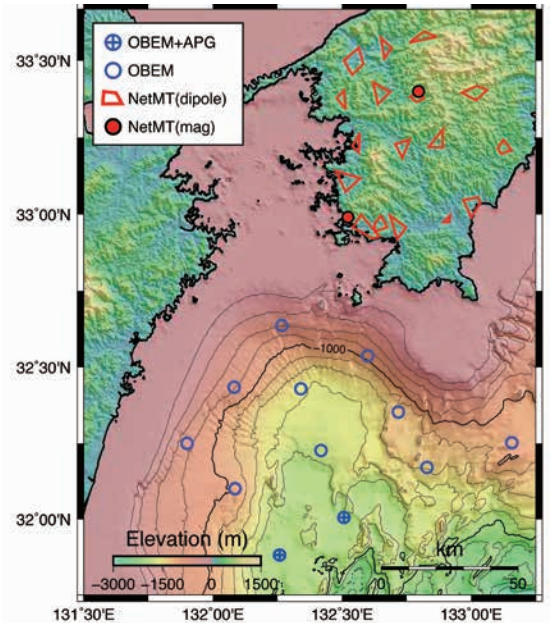

Fig. 1. Study area, with the locations of the onshore (red) and offshore (blue) MT observation sites shown.

Here we show the results from April to May 2016. We first examine two NNW–SSE-oriented cross-sections that lie within (**Fig.2b**) and outside of (**Fig.2c**) the slow slip event (SSE) area. Significant low-resistivity anomalies are detected in the middle crust of the hanging wall of the subducting Philippine Sea slab in both cross-sections. Earthquakes tend to occur in the high-resistivity area, avoiding those low-resistivity anomalies, with previous studies obtaining similar results in other areas (e.g. Ichihara *et al.*, 2014; Hata *et al.*, 2018). However, no remarkable conductive anomaly is imaged around the subducting slab due to these shallower conductive anomalies, which make it difficult to resolve the resistivity distribution at depth. We examine the section parallel to the slab surface by comparing the resistivity structures to the seismic attenuation (Q_p) structures (Kita and Matsubara, 2016) to clarify the relationship between the resistivity structure and SSE area. A positive correlation between both parameters is detected. The mantle wedge above the slab in the SSE area is relatively resistive and possesses a high-Q_p structure, whereas the mantle wedge above the slab and outside of the SSE area is relatively conductive and possesses a low-Q_p structure. This resistive and high-Q_p layer may indicate an impermeable layer that confines the fluids along the subducting slab. The confined fluids may cause SSEs; however, we cannot explicitly image the confined fluids as the conductive anomaly from the current dataset.

Marine-MT survey

Marine-MT surveys have been conducted since March 2017 at twelve sites around the offshore Miyazaki and Kochi areas, Japan, using ocean bottom electromagnetometers (OBEMs) (**blue circles in Fig.1**). The T/S *Fukae-maru*, which is owned by Kobe University, oversaw the deployment and recovery of the OBEMs. Absolute pressure measurements were also acquired at two OBEM sites to detect SSEs. High-quality frequency-domain response functions between the voltage difference and magnetic field were estimated, especially for the data in 2017, when a high level of solar activity was observed.

Preliminary forward 3-D resistivity modeling indicates that the estimated response functions are sensitive to the resistivity anomaly around the plate interface beneath the OBEMs. We are now estimating the 3-D resistivity distribution using 3-D inversion methods.

Future work

We intend to investigate the temporal changes in the resistivity structure along the top of the slab since significant SSEs have recently occurred in the study area. We also plan to combine the Network- and marine-MT data to obtain a reliable resistivity structure that covers the SSE areas in the western Nankai subduction zone.

Acknowledgements

We acknowledge the staff at the Nippon Telegraph and Telephone WEST Corporation and related companies for their cordial support during the Network MT-survey. We also acknowledge the T/S *Fukae-maru* ship crew for their support and assistance during the OBEM survey.

References

Hata, M., *et al.* (2018), *JGR* 123: 6334-6346, doi:10.1029/2018JB015951

Ichihara, H., *et al.* (2014), *EPS* 66: 50, doi:10.1186/1880-5981-66-50

Kita, S., Matsubara, M. (2016), *JGR* 121:1962–1982. doi:10.1002/2015jb012493

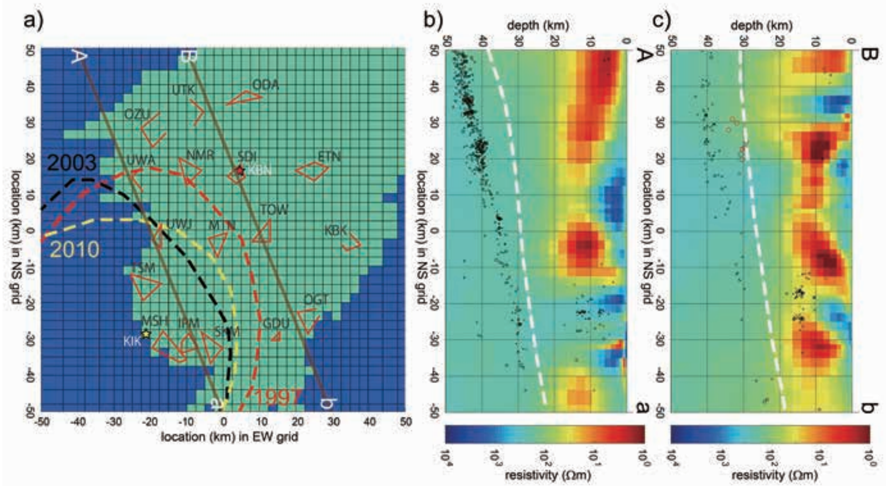

Fig. 2.
a) Distribution of the Network-MT dipoles (red lines), magnetic stations (stars), and areas of three recent long-term SSEs (dashed red curve: 1997; dashed black curve: 2003; dashed yellow curve: 2010; cumulative slip >10 cm; after a report by GSI at the 205th meeting of the CCEP, 2014). b) and c) Resistivity distribution along Lines A–a and B–b in Fig. 2a, respectively. The hypocenters of the normal (black circles) and low frequency (red circles) earthquakes, which are taken from the Japan Meteorological Agency catalog, are shown. The dashed white line denotes the top of the subducting Philippine Sea slab.

Introduction to Research in Group B02

Migration of slow earthquakes driven by fluid flow ?

Ikuo KATAYAMA, Faculty of Science, Hiroshima University

One of the unique characteristics of slow earthquakes occurring at plate-convergent regions is the slow migration of low-frequency tremor (e.g., Obara, 2002; Ghosh *et al.*, 2010). Such a migration process is likely associated with fluid flow along the subducting plate interface, since the occurrence of slow earthquake is closely related to the presence of aqueous fluids. Based on our recent laboratory experiments (Katayama *et al.*, 2018), we discuss how the migration of slow earthquakes relates to fluid flow along the subducting plate interface.

We conducted fluid-induced fracturing experiments on intact granite to investigate the relationship between the fracturing process, and pore pressure build-up and fluid diffusion. Acoustic events and macroscopic failure in the sample were triggered by the pore fluid pressure build-up, with fracturing occurring when the average effective stress reached a critical stress state, following the Mohr-Coulomb failure criterion. The spatiotemporal distribution of acoustic events is mainly controlled by the pore pressure diffusion front through the sample, with diffusion coefficient of ~10^{-6} m^2/s estimated based on the migration of acoustic emissions (**Fig.1a**). This value is nearly consistent with the hydraulic diffusivity (D), which is calculated from the permeability (k), as follows:

$$D = \frac{k}{\eta(\phi\beta_f + \beta_r)}$$

where η is the fluid viscosity, ϕ is the porosity, and β_f and β_r are the compressibilities of the fluid and rock, respectively. This agreement suggests that the

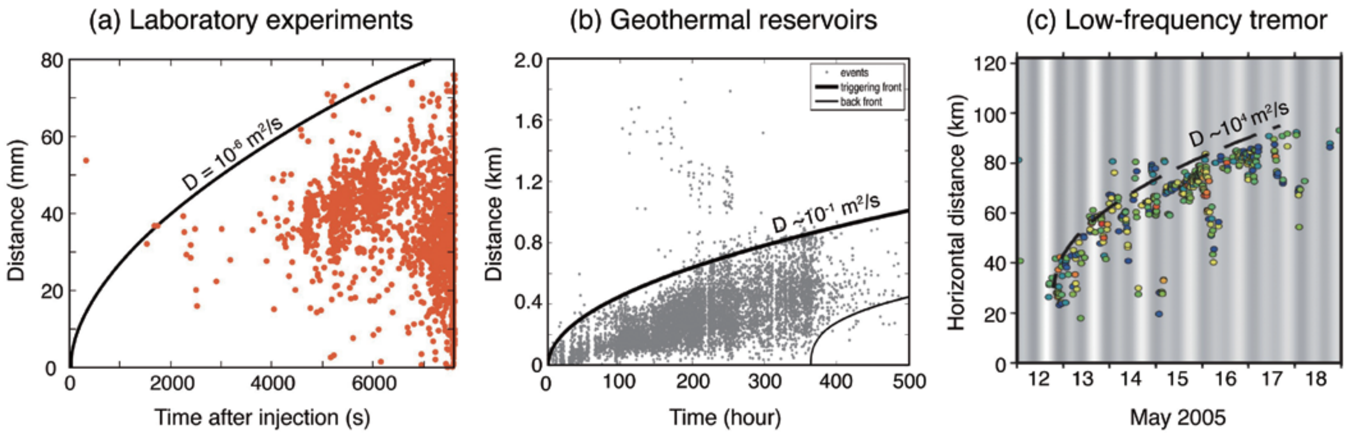

Fig. 1.
Hydraulic diffusivity (*D*) measurements in various environments. (a) Laboratory fracture experiments in granite specimens (Katayama *et al*., 2018). (b) Fluid injection tests in geothermal reservoirs (Shapiro and Dinske, 2009). (c) Migration of low-frequency tremors (Ide, 2010).

migration of acoustic events is mainly controlled by fluid diffusion through the sample.

A similar parabolic diffusive migration has been reported in other studies, such as fluid injection tests in geothermal reservoirs (Shapiro and Dinske, 2009) and slow earthquakes at subduction zones (Ide, 2010) (**Figs.1b and c**). However, the inferred diffusion coefficients in these environments are significantly larger than that for the laboratory experiments, which values of ~10^{-1} m^2/s for the fluid injection tests and ~10^4 m^2/s for slow earthquakes. This difference may be attributed to the scaling problem, as the permeability is known to be much larger in natural settings than in laboratory experiments. Furthermore, the fluid viscosity can be significantly lower in both the geothermal reservoir and the souse regions of slow earthquakes due to the supercritical condition of aqueous fluids. These differences in permeability and fluid viscosity can explain the variations in hydraulic diffusivity, suggesting that the migration of slow earthquakes may result from slow crack nucleation and growth controlled by pore pressure diffusion along the subducting plate interface (**Fig.2**). However, this is still a working hypothesis, and other processes, such as the stress transfer across a heterogeneous asperity contact, are potential alternative mechanisms that can explain the slow migration of low-frequency tremors. If we can monitor fluid migration along the plate interface using geophysical data, such as electrical resistivity and seismic attenuation measurements, then we can better understand the migration mechanism of slow earthquakes, which may provide an insight into the key processes that influence the occurrence of slow earthquakes.

References

Ghosh, A., *et al*. (2010), *Geochem. Geophys. Geosys.* 11, doi:10.1029/2010GC003305.

Ide, S. (2010), *Nature* 466, 356–359, doi:10.1038/nature09251.

Katayama, I., *et al*. (2018), *Geophys. Res. Lett.* 45, 7488–7495, doi:10.1029/2018GL077815.

Obara, K. (2002), *Science* 296, 1679–1681, doi:10.1126/science.1070378.

Obara, K., and Kato, A. (2016), *Science* 356, 253-257, doi:10.1126/science.aaf1512.

Shapiro, S. A., and Dinske, C. (2009), *Geophys. Prospect.* 57, 301–300, doi:10.1111/j.1365–2478.

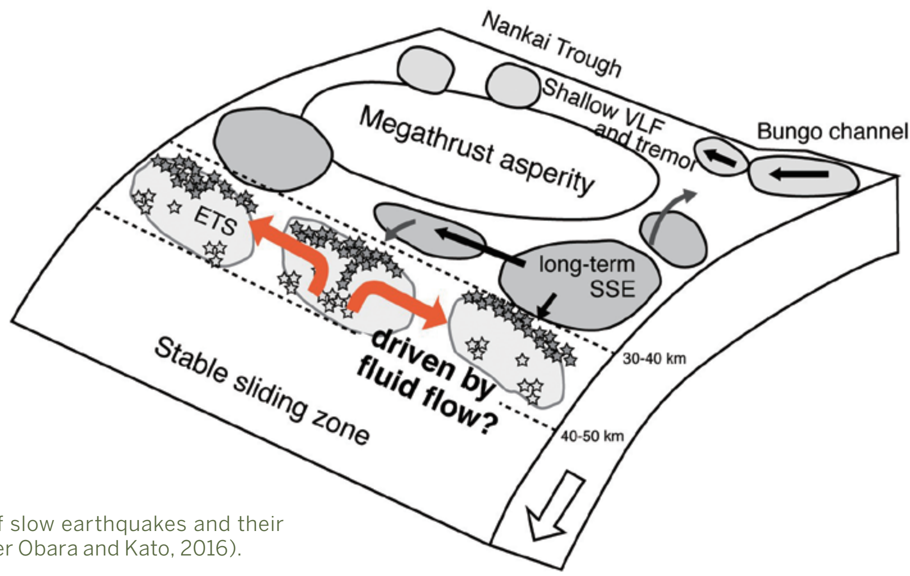

Fig. 2.
Occurrence of slow earthquakes and their migration (after Obara and Kato, 2016).

Introduction to Research in Group C01

Inferences on the source mechanism of slow earthquakes from statistical characteristics

Masaru NAKANO, Research Institute for Marine Geodynamics, Japan Agency for Marine-Earth Science and Technology

The size distribution of ordinary earthquakes largely follows a power law, whereby the earthquake frequency is proportional to its size on a logarithmic scale. This relation is known as the Ishimoto–Iida or Gutenberg–Richter (GR) law. The proportionality constant is represented by the b-value, which is about one, but its variability is related to changes in the stress state around the source. For example, the b-value generally decreases as the stress level increases, and vice versa. However, some types of volcanic earthquakes follow an exponential law, whereby the logarithm of the earthquake frequency is proportional to its size. This size distribution may reflect the source mechanism: Events that follow a power-law size distribution may be self-similar, whereas a characteristic scale may exist for events that follow an exponential-law size distribution. We can therefore investigate the source mechanism from the earthquake size distribution, which can also be used as a benchmark for theoretical slow earthquake models.

Which size distribution do slow earthquakes follow? Some studies have obtained a power-law distribution for deep low-frequency tremor, while others have obtained an exponential-law distribution. Very-low-frequency earthquakes and slow-slip events largely follow a power-law size distribution.

Slow earthquakes also occur along the Nankai Trough, southwest of Japan, where ocean-bottom seismometers have detected these slow events on the shallower part of the plate interface, beneath the accretionary prism (**Fig.1**). Here we investigate the size distribution of shallow tremor. The earthquake size is generally measured by its seismic moment, which is estimated from the amplitudes of the long-period components. However, the long-period component of tremor signals is generally below the noise level, which makes it extremely difficult to accurately compute the seismic moment. Recent studies have demonstrated that the seismic energy computed from the short-period components of tremor signals is proportional to the seismic moment (Ide and Yabe, 2014; Yabe *et al*., 2019). This approach allows us to obtain the size distribution of shallow tremor from the observed seismic energy (Nakano *et al*., 2019).

The obtained tremor size distribution largely follows a power law, with b-values between 1 and 1.3 (**Fig.2**). However, the event frequency is smaller than expected for the largest events, such that an exponential law provides a better fit to these larger events. Such a distribution is called the tapered Gutenberg-Richter

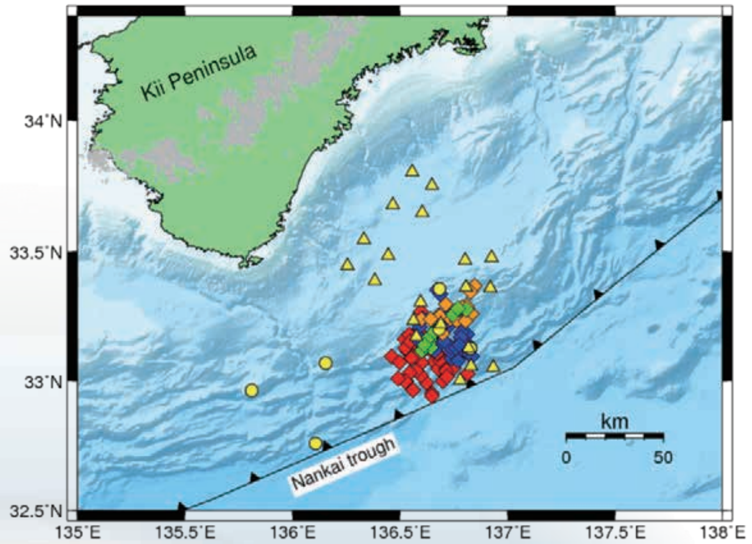

Fig. 1.
Distribution of shallow tremor in the Nankai Trough off the Kii Peninsula. Diamonds mark the locations of the daily average tremor sources for 2009 (red), 2015 (green), 2016 (blue), and 2018 (orange). Yellow circles and triangles represent BBOBS (2008–2009) and DONET (2011–) stations, respectively. Gray dots represent the deep tremor locations (Maeda and Obara, 2009; Obara *et al*., 2010).

(TGR) distribution (Kagan, 2002), and it explains the observations well (**green curves in Fig.2**). A possible explanation for this observed distribution is that small events are self-similar, following a power-law size distribution, whereas the largest events follow an exponential-law distribution due to a potential limit to the source size. Another possible cause for the exponential taper is slip braking due to viscous friction, which suppresses event growth.

Here we investigated the size distribution of shallow tremor. Studies investigating other statistical characteristics, as well as those that combine theoretical models and experimental studies, would further improve our understanding of slow earthquake source mechanisms.

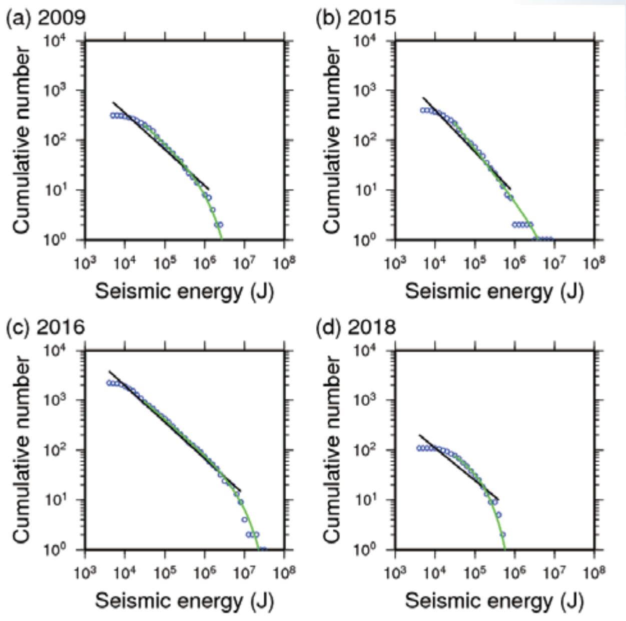

Fig. 2.
Size distribution of shallow tremor (blue circles) in (a) 2009, (b) 2015, (c) 2016, and (d) 2018. The Black lines and green curves are the best-fit GR and TGR distributions to the observations, respectively.

References

Kagan, Y. Y. (2012), *Geophys. J. Int.* 148, 520-541, doi:10.1046/j.1365-246x.2002.01594.x.

Ide, S., and Yabe, S. (2014), *Geophys. Res. Lett.* 41, 2786–2793, doi:10.1002/2014GL059712.

Maeda, T., and Obara, K. (2009), *J. Geophys. Res.* 114, B00A09, doi:10.1029/2008JB006043.

Nakano, M., *et al.* (2019), *Geophys. Res. Lett.* 46, 5828–5836, doi:10.1029/2019GL083029.

Obara, K., *et al.* (2010), *Geophys. Res. Lett.* 37, L13306, doi:10.1029/2010GL043679.

Yabe, S., *et al.* (2019), *J. Geophys. Res.* 124, 1507–1519, doi:10.1029/2018JB016815.

Introduction to Research in Group C02

Simplified slow earthquakes: Finding the minimum model for understanding slow earthquakes

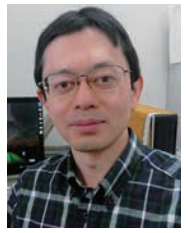

Takehito SUZUKI, Dept. Phys. & Math., Aoyama Gakuin University

Our knowledge of slow earthquakes and their associated processes is largely based on observational and modeling studies, with large and focused projects, such as "Science of Slow Earthquakes," pushing the envelope in advancing our understanding of these earthquake phenomena. Many observational results have been obtained, and numerous theoretical models have been proposed to explain these results. However, it should be emphasized that the theoretical approaches should not concentrate on reproducing the detailed behavior of slow earthquakes. We should rather focus on determining the minimum model that allows us to understand slow earthquake processes.

Here we replace the fault motion with an infinitely long block that is pushed along a substrate (Suzuki and Matsukawa, 2019). This is obviously a significant simplification, and it cannot describe the fault motion in detail. However, we can consider this the simplest dynamic earthquake slip model. This allows us to use the differences between steady slip and creep motion as an analogue for the differences between ordinary and slow earthquakes.

We focus on the slip velocity profile for the steady-state condition with a slip-front-propagation velocity

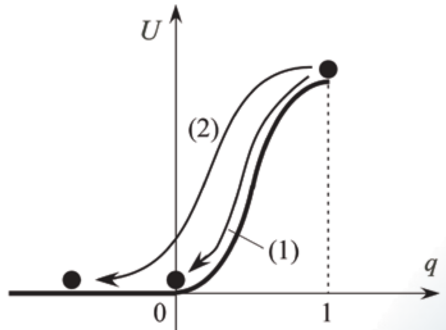

Fig. 1.
Motion in the potential. Case (1) corresponds to the critical case, and case (2) represents the slip behavior when the boundary strain is larger than the critical value.

v in the present model. We consider an infinitely long visco-elastic block on a substrate, which can be regarded as a one-dimensional model along the x-axis. We assume a friction law with a quadratic form of the slip velocity:

$$\begin{aligned}\tau &= a\dot{u}(2b-\dot{u})[H(\dot{u})-H(\dot{u}-2b)]\\ &= a\dot{u}(v_{\mathrm{van}}-\dot{u})[H(\dot{u})-H(\dot{u}-v_{\mathrm{van}})],\end{aligned} \tag{1}$$

where u is the displacement, a and b are positive constants, H is the Heaviside step function, $v_{\mathrm{van}}=2b$ is the slip velocity at which τ vanishes, and the dot represents temporal differentiation. This friction law is based on experimental results that have suggested negligible dynamic friction coefficients for the high-speed slip region (e.g., Di Toro *et al.*, 2011). The normalized governing equation (e.o.m.) is given by:

$$\begin{aligned}\ddot{u} &= u'' + \dot{u}'' - a\dot{u}(v_{\mathrm{van}}-\dot{u})\\ &\quad\times[H(\dot{u})-H(\dot{u}-v_{\mathrm{van}})].\end{aligned} \tag{2}$$

Note that the Young's modulus and the viscosity are normalized, and the prime notation represents spatial differentiation. The steady-state solution for Eq. (2) with propagation velocity v satisfies the equation:

$$\begin{aligned}&(1-v^2)u'' - vu''' - avu'(vu'+v_{\mathrm{van}})\\ &\quad\times\left[H(u')-H\left(u'+\frac{v_{\mathrm{van}}}{v}\right)\right],\end{aligned} \tag{3}$$

where the prime notation represents differentiation with respect to $x_1 = x - vt$. Deformation causes Eq. (3) to reduce to:

$$\begin{aligned}\frac{\partial^2 q}{\partial X^2} &= -\mu\frac{\partial q}{\partial X} - \frac{\partial}{\partial q}\left(\frac{q^2}{2}-\frac{q^3}{3}\right)\\ &\quad\times[H(q)-H(q-1)],\end{aligned} \tag{4}$$

where $q=(v/v_{\mathrm{van}})(u'+v_{\mathrm{van}}/v) = -(\dot{u}-v_{\mathrm{van}})/v_{\mathrm{van}}$, $X=-x_1\sqrt{av_{\mathrm{van}}}$, and $\mu=(1-v^2)/(\sqrt{av_{\mathrm{van}}}v)$. If we regard the differentiation with respect to X as that with respect to the time in Eq. (3), then Eq. (4) is equivalent to the e.o.m. for a particle with a unit mass under the potential $U=q^2/2-q^3/3$ and a damping force that is proportional to the velocity, $-\mu\partial q/\partial X$. Here we consider the slip velocity profile with $\dot{u}=v_{\mathrm{van}}$ at $x_1\to-\infty$ and $\dot{u}=0$ at $x_1\to\infty$. This profile is equivalent to the motion for $q(X\to-\infty)=1$ and $q(X\to\infty)=0$, where U takes the maximum and minimum values, respectively, in Eq. (4) [case (1) in **Fig.1**]. We also note that μ is the quantity to be determined in Eq. (4), and it has a critical value μ_c. If $\mu<\mu_c$, then the particle can approach the region $q>0$ as $X\to\infty$. Therefore, the case $\mu=\mu_c$ corresponds to the boundary condition where $\dot{u}=v_{\mathrm{van}}$ at $x_1\to-\infty$. Furthermore, $\mu_c=2$ has already been obtained for U (Aronson and Weinberger, 1975). Therefore, the condition $\mu=(1-v^2)/(\sqrt{av_{\mathrm{van}}}v)=2$ yields the propagation velocity $v=\sqrt{1+g}-\sqrt{g}$, where $g\equiv|\partial\tau/\partial\dot{u}|_{\dot{u}=v_{\mathrm{van}}}|=av_{\mathrm{van}}$. It should be emphasized that the gradient of the $\tau-\dot{u}$ curve at $\tau=0$ completely determines the propagation velocity.

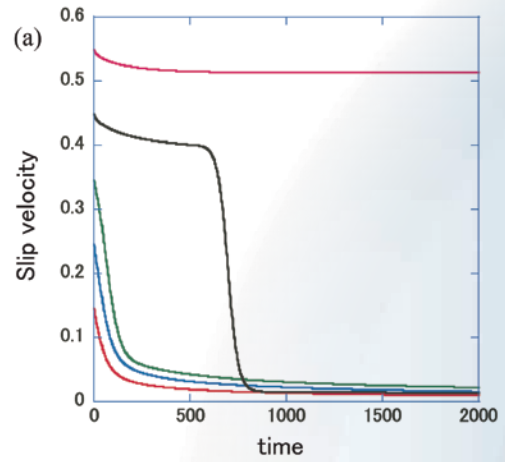

Fig. 2.
Slip velocity as a function of time for various initial strains. The $|p_c|$ value is 0.461, and the initial strains in the model (at t=0) are 0.55 (purple), 0.45 (black), 0.35 (green), 0.25 (blue), and 0.15 (red).

The above-mentioned boundary condition ($\dot{u}=v_{\mathrm{van}}$ at $x_1\to-\infty$) is the critical one. It should also be noted that the absolute value of the normal strain given at $x_1\to-\infty$ for the critical case, $|p_c|=v_{\mathrm{van}}/v$, is also the critical value. Macroscopic steady-state slip occurs when the strain is larger than this value, whereas steady-state slip does not occur when the strain is smaller than this value. The latter behavior can be regarded as creep-like motion. Furthermore, the condition $\dot{u}>v_{\mathrm{van}}$ is satisfied at $x_1\to-\infty$ for the former case [case (2) in **Fig.1**], and the propagation velocity is larger than $\sqrt{1+g}-\sqrt{g}$. Therefore, we can conclude that $v=\sqrt{1+g}-\sqrt{g}$ is the minimum propagation velocity for steady state. **Figure 2** shows both cases: steady slip is observed for the case $|p_c|=0.55$, whereas such slip does not appear for the other cases. We may consider that the former case corresponds to ordinary earthquakes, whereas the latter case explains slow earthquakes. Furthermore, this result implies that the propagation velocity for slow earthquakes does not exceed $\sqrt{1+g}-\sqrt{g}$.

We have also confirmed that our result can be applied to the cases where the $\tau-\dot{u}$ curve is not a parabola and τ does not vanish in the high-$\dot{u}$ region, although we omit these results in our discussion. We find that the simplest model only requires g to determine the propagation velocity. While current seismological models often use many model parameters, our simple earthquake model can yield many physical implications.

References

Aronson, D. G., and Weinberger, H. F. (1975), *J. A. Goldstein, ed.*, Partial Differential Equations and Related Topics, Lecture Note in Math., 466, Springer, 5-49.

Di Toro, G., *et al.* (2011), *Nature* 471, 494, doi:10.1038/nature09838.

Suzuki, T., and Matsukawa, H. (2019), *J. Phys. Soc. J.* 88, 114402, doi:10.7566 / JPSJ.88.114402.

Introduction to Publicly Offered Research in Group A01

Mathematical modeling of slow earthquakes based on the inter-event time and amplitude distribution

Akiko TAKEO, ERI, UTokyo

I focused on the inter-event time and amplitude distributions of very low frequency earthquakes that occurred episodically as swarms every several months to years in the Nankai subduction zone to reveal the physical process of slow earthquakes. I detected thousands of very low frequency earthquakes by combining the waveforms from permanent stations and new stations deployed by the "Science of Slow Earthquakes" project (Fig.1). The amplitude distributions of the shallow seismicity near the Nankai Trough can be explained by an exponential curve that possesses a characteristic earthquake size (Fig.2). Furthermore, the distribution of inter-event times differs from that of mainshock–aftershock sequences of regular earthquakes. However, the deep very low frequency earthquakes are small in magnitude, and an evaluation of the amplitude distribution is difficult. I used these results to design a broadband seismic station distribution in 2019–2020 by the A01 group of the "Science of Slow Earthquakes" project (Fig.1), with the goal of detecting smaller events.

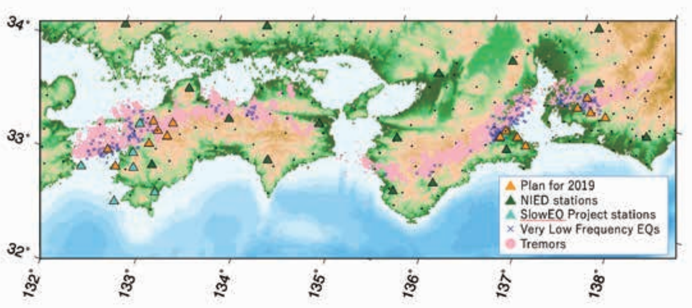

Fig. 1.
Broadband seismometer array design developed by the "Science of Slow Earthquakes" project.

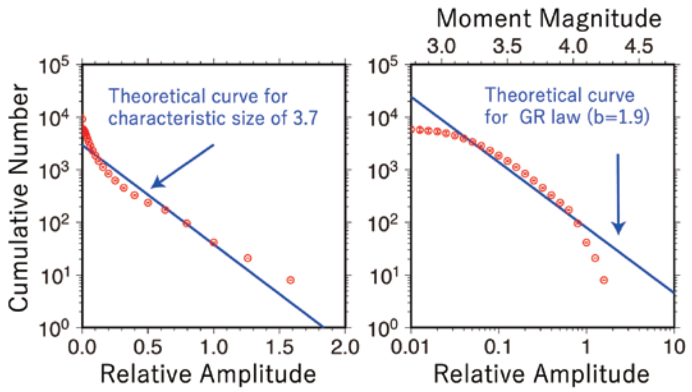

Fig. 2.
Size distribution of shallow very low frequency earthquakes. The blue lines represent an exponential curve (left) and the theoretical Gutenberg–Richter relationship (right).

Introduction to Publicly Offered Research in Group A02

Detection of inland slow slip corresponding to earthquake swarms

Mako OHZONO, Hokkaido Univ.

The possibility of a shallow slow-slip event (SSE) in the inland region of northern Hokkaido, Japan, has recently been reported using a dense Global Navigation Satellite System (GNSS) network (Ohzono *et al.*, 2015). This event occurred at the same time as M4-class earthquake swarm activity. This event presents a rare case since most slow earthquakes have been detected on the plate interface at subduction zones.

The Japan Meteorological Agency (JMA) hypocenter catalogue and GEONET GNSS data across Japan are analyzed from October 1997 to December 2016 to determine if other SSEs have occurred and better understand their mechanism. In this study, a swarm area is defined as an area that experiences more than three $M \geq 4.0$ earthquakes a year. The baseline length changes in the GNSS data around these areas are then analyzed to determine whether transient surface deformation occurred (Fig.1).

Nineteen swarm areas are detected, with transient baseline changes corresponding to the swarms observed in six areas. However, it is difficult to estimate the degree of aseismic fault slip because the transient deformation signals are small compared with the case of northern Hokkaido, and the GNSS site distribution is currently inadequate to fully distinguish the deformation signals.

However, there is still room for improving this method to detect transient signals. A more detailed data analysis of both the seismic and GNSS data, as well as other geophysical information, will potentially increase the number of cases of inland SSEs.

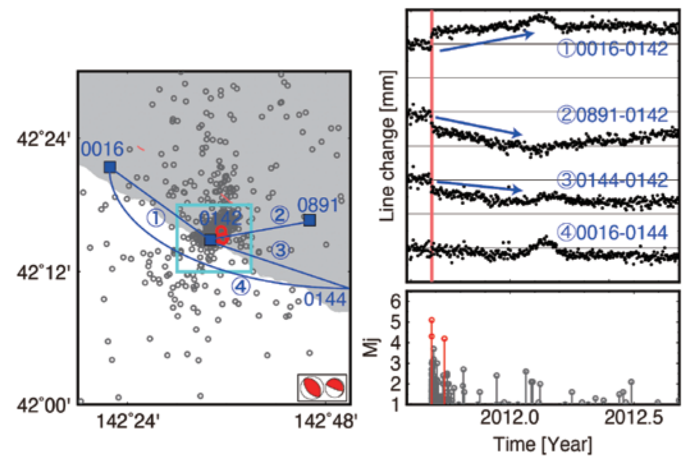

Fig. 1.
Example of a transient GNSS baseline length change in the Hidaka region, Hokkaido. (a) Hypocenter distribution (JMA catalog) and GNSS site locations. (b) Baseline length changes around the swarm area. The four baseline locations are shown in (a). The red line marks the timing of the first $M \geq 4$ earthquake. (c) M–t diagram for the area within the light-blue square in (a). The $M \geq 4$ events are shown in red.

Introduction to Publicly Offered Research in Group A02

Periodic changes in interplate locking off Kyushu Island, Southwest Japan

Takeshi IINUMA, JAMSTEC

There are temporal variations in the occurrence of long-term slow-slip events that occur on the plate interface between the Philippine Sea Plate subducting from the Nankai Trough and the overriding continental plate due to changes in the interplate locking state. We applied the monitoring method proposed by Iinuma (2018, *GJI*), which utilizes temporal changes in the spatial gradients of the surface displacement rate field obtained from terrestrial Global Navigation Satellite System (GNSS) observations, to GNSS data from Southwest Japan to investigate the spatiotemporal changes in the degree of interplate locking. We compared the results with temporal changes in the interplate slip rate estimated from the small repeating earthquakes that occur on the plate interface, and found that the periods when the slip rate accelerated and decelerated coincided with the periods when the spatial gradients in the GNSS data were positive and negative, respectively (Fig.). This suggests that there are frequency-dependent periodic changes in the degree of interplate locking on the plate interface off Kyushu Island that are similar to those revealed by Uchida *et al.* (2016, *Science*) along the northeast Japan subduction zone.

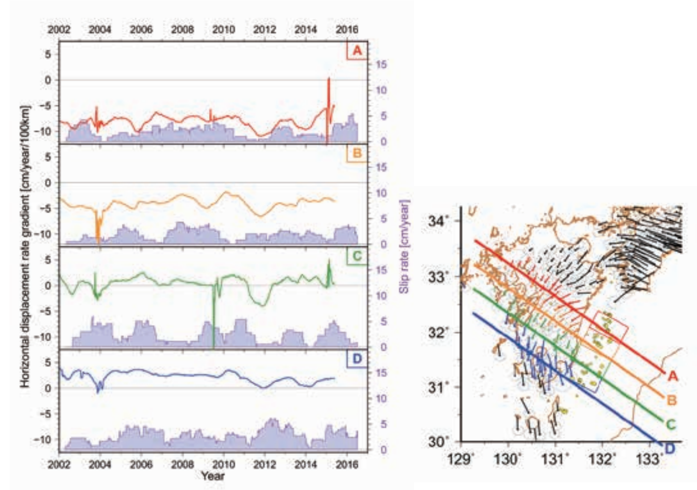

Fig. (Left) Time series of the spatial gradient of the surface horizontal displacement rate gradient along each swath (red, orange, green, and blue lines, with the swath locations shown in the right panel), and slip rate estimated from the small repeating earthquakes in each area (purple filled lines).
(Right) Horizontal surface displacement rate field during the January 2009–January 2011 period. The swaths used to calculate the spatial gradients of the displacement rate field in the left panel are shown as the thick colored lines, and the areas used to estimate the slip rate based on the small repeating earthquakes in the left panel (yellow circles in the colored rectangles) are also shown.

Introduction to Publicly Offered Research in Group A02

Utilization and improvement of OBP data for the detection of SSEs

Yusaku OHTA, Tohoku Univ.

Seafloor geodetic techniques play an important role in detecting and understanding the variety of slow-slip events (SSEs) that occur along the subducting plate interface due to the relative insensitivity of onshore geodetic networks. For example, an ocean bottom pressure (OBP) gauge measures the water pressure. Therefore, an OBP system can detect both a tsunami and vertical seafloor displacements. Tohoku University has been successful in detecting both the pre- and postseismic crustal deformation of the 2011 Tohoku Earthquake using an OBP system.

However, there are several problems that still need to be addressed regarding OBP systems. For example, the non-tidal component in the ocean current may affect OBP records. The long-term sensor drift of the pressure sensors equipped with OBPs has also been a serious and long-standing problem for the detection of slow crustal deformation.

One approach to reducing the long-term drift from OBP records is the so-called "A-0-A" method. This method uses the atmospheric pressure in the housing as the reference pressure instead of a pressure standard, such as a dead-weight tester, to monitor the sensor drift. We conducted a series of laboratory experiments with the pressure standard at the National Institute of Advanced Industrial Science and Technology (AIST), Japan, to assess the "A-0-A" approach. We determined that the drift characteristic can basically be removed by treating the atmospheric pressure as a zero-point ("0") (Fig.1).

We are now developing a new OBP prototype with the "A-0-A" function, which can be deployed in deep-sea (~6,500 m) environments. This new system is expected to improve our ability to acquire more robust SSE observations.

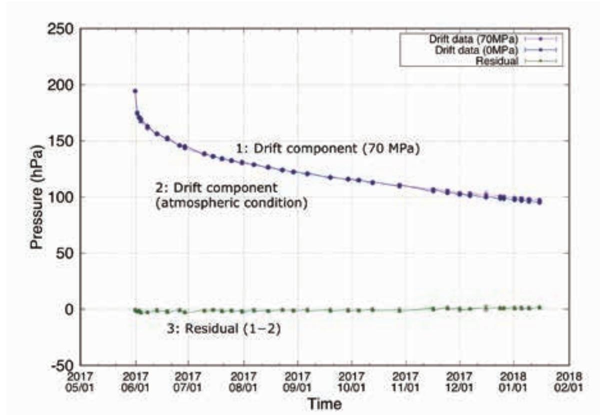

Fig. 1.
Obtained time series in the laboratory experiment. The "A-0-A" approach can basically remove the sensor drift.

Introduction to Publicly Offered Research in Group B01

Plate coupling controlled by the three-dimensional fluid distribution along the Hikurangi subduction zone, New Zealand

Yasuo OGAWA, Tokyo Tech.

The northeastern part of the North Island, New Zealand, has weak plate coupling and is a zone where slow earthquakes commonly occur, whereas the southern part of the North Island has strong plate coupling and a locked plate interface. Napier, on the eastern coast of the North Island, appears to mark where this transition in plate coupling occurs, with a gradual transition from weaker to stronger plate coupling to the south. The Tokyo Institute of Technology and GNS Science (New Zealand) have acquired a dense grid of magnetotelluric (MT) measurements at 160 sites across this region, and analyzed the resistivity structure in three dimensions (Fig.1). We focus on modeling the resistivity distribution above the subducting plate by fixing the resistivity of the subducting plate at 1,000 Ωm. We then compare the model results with areal strain velocity measurements (Fig.2). We generally find (1) lower resistivities in the northeast, where the areal strain velocity is higher, and (2) higher resistivities in the southwest, where the areal strain velocity is lower. We also observe a low-resistivity anomaly at the northeastern corner of our model space that is consistent a positive areal strain anomaly. These results support the hypothesis that the fluid distribution at the subducting plate interface controls plate coupling.

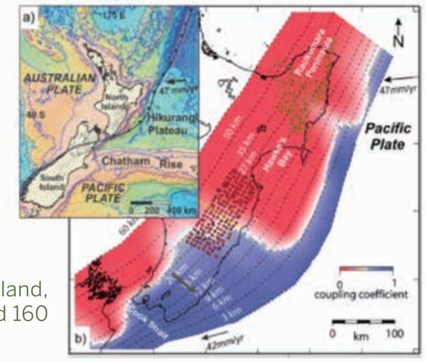

Fig. 1.
(a) North Island, New Zealand, and (b) plate coupling and 160 MT stations (red dots).

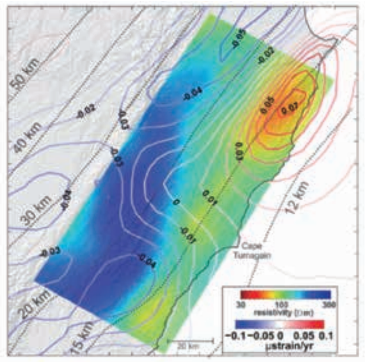

Fig. 2.
Resistivity distribution above the subducting plate, along with contours of the areal strain velocity.

Introduction to Publicly Offered Research in Group B02

Evolution of the frictional properties of incoming hemipelagic sediments during diagenetic reactions

Keishi OKAZAKI, JAMSTEC

There has been a growing interest in understanding the influence of diagenesis following dehydration reactions on regular and slow earthquakes in subduction zones. Here we study the effects of diagenetic reactions on the frictional properties of incoming hemipelagic sediments that were collected along the NE Japan subduction zone during the KS-15-3 Shinseimaru cruise. Our friction experiments are conducted at a 150 MPa confining pressure (P_c), 58 MPa pore fluid pressure (P_p), and 25–230°C temperature range (T). When the samples were immediately sheared after reaching the temperatures ranging 25–100°C, the frictional behaviors exhibit velocity-strengthening (i.e., positive $a-b$ value) (Fig.1a). The $a-b$ value is negative at T > 150°C. An oscillatory behavior is observed at 200°C, whereas stick–slip behavior is observed at 230°C (Fig.1a). We also conduct "cook and kick" experiments to evaluate effects of the time-dependent diagenetic reactions on the frictional properties of the hemipelagic sediments. Velocity-weakening is observed after "cooking" the sediments at 100°C, P_c = 100 MPa, and P_p = 58 MPa for 3 × 10⁴ s (8h) (Fig.1b). Extrapolation of the Arrhenius law suggests that the velocity-strengthening to weakening transition occurs at T = 60–80°C on a geological timescale. These diagenetic reactions may determine both the upper limit of the seismogenic zone and the source region of low-frequency earthquakes.

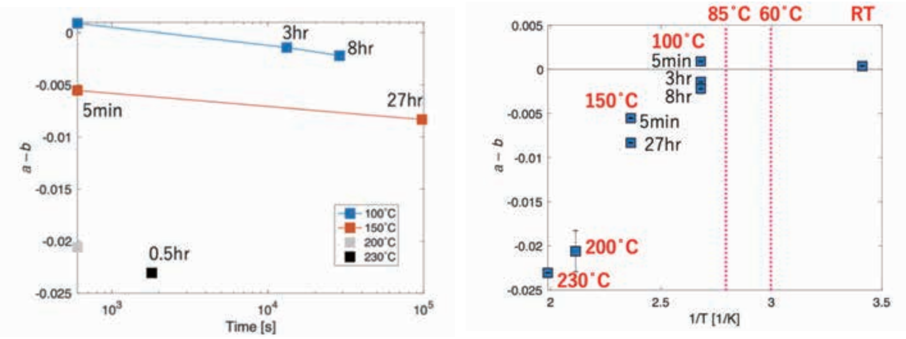

Fig. 1.
Velocity dependence of the friction coefficient ($d\mu/d\ln V = a - b$). (a) Experimental results after cooking. (b) Arrhenius-type temperature dependence of the results.

Introduction to Publicly Offered Research in Group B02

Aseismic–seismic transition in faulting around the seismogenic updip limit of subduction zones

Kyuichi KANAGAWA, Chiba Univ.

Friction experiments on opal, which is a main component in chert on the Pacific Plate subducting at the Japan Trench off Tohoku, suggest that the increasing activity of the pressure solution and/or decreasing displacement rate with increasing temperature promotes gouge lithification, which increases the steady-state friction coefficient μ_{ss}. (Fig.1a). This increase in μ_{ss} leads to a decrease in its velocity dependence $d\mu_{ss}/d(\ln V)$, with $d\mu_{ss}/d(\ln V) = 0$ marking the updip limit of seismogenic faulting along subduction-zone megathrusts (Fig.1b). Furthermore, friction experiments on accretionary sediments and rocks reveal that the transition temperature from aseismic to seismic faulting is different among the analyzed rock types (Fig.1c).

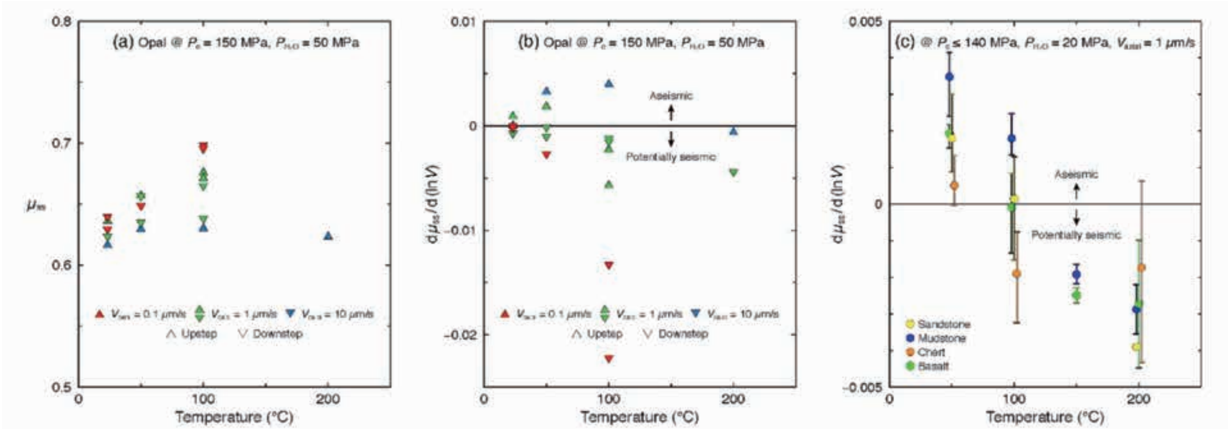

Fig. 1.
(a) Steady-state friction coefficient μ_{ss} and (b) its velocity dependence $d\mu_{ss}/d(\ln V)$ in opal gouge plotted against temperature. (c) $d\mu_{ss}/d(\ln V)$ of various accretionary sediments and rocks plotted against temperature (c). The experimental conditions are provided on each plot.

Introduction to Publicly Offered Research in Group C01

Migration of aqueous fluids within a thin, low-viscosity layer on top of a subducting slab

Manabu MORISHIGE, JAMSTEC

Aqueous fluids play critical roles in the generation of slow earthquakes. Most previous studies, however, have focused only on "where" and "how much" these fluids are released in the slab, such that the subsequent aqueous fluid migration is relatively unknown. Here I aim to understand the fluid migration mechanisms near the subducting plate interface based on a two-phase flow model, which allows us to simultaneously treat the movement of the rock and fluid phases. I investigate the behavior of aqueous fluids within a thin, low-viscosity layer (LVL) on top of a subducting slab. The results demonstrate that (1) a large amount of the fluids are efficiently trapped in the LVL due to compaction effects, and (2) the fluids migrate upward through the LVL due to the dynamic pressure gradient caused by shear deformation of the LVL (Fig.1). I also observe spatial variations in the fluid volume fraction, which is a characteristic behavior of fluid migration through a viscously deformable, permeable solid. These findings may help us better understand the observed spatiotemporal variations in slow earthquakes.

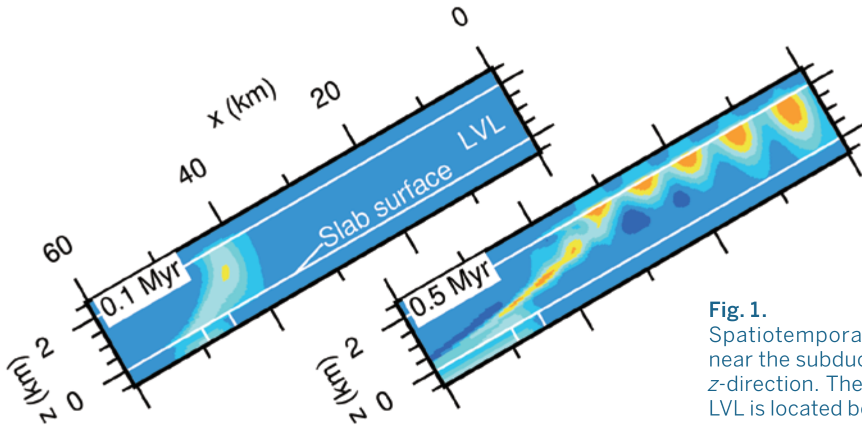

Fig. 1.
Spatiotemporal variation in the volume fraction of aqueous fluids near the subducting plate interface. Each figure is exaggerated in the z-direction. The hot colors indicate a large fluid volume fraction. The LVL is located between z = 0 and 2 km.

Introduction to Publicly Offered Research in Group C02

Nonlinear stress–strain response in systems with different time scales

Michio OTSUKI, Osaka Univ.

Fragile materials, including sands, colloidal suspensions, and foams, exhibit nonlinear stress–strain responses (e.g., fracture, slip, and yield). This behavior is usually due to the combination of slow changes in the external field and an abrupt transition in the internal components of the material. There is currently no unified understanding of this nonlinear response, even though many researchers have investigated such a response. Therefore, we investigated frictional granular materials under sufficiently slow shear to understand the mechanism shaping this nonlinear response.

It has been reported that the shear modulus G of frictionless granular materials exhibits a continuous transition above a critical packing fraction, which is called the jamming point. However, intergranular friction exists in granular materials, and we cannot neglect its effect. Therefore, we have numerically investigated the stress–strain response of frictional grains under shear stress, and found that G exhibits a discontinuous transition, even at the frictionless limit (Fig.1). This behavior appears to contradict previous studies, but we note that this is only observed when the strain is infinitesimal and the nonlinear response under finite strain corresponds to the continuous transition in frictionless grains. This nonlinear behavior is due to intermittent microscopic intergranular slip.

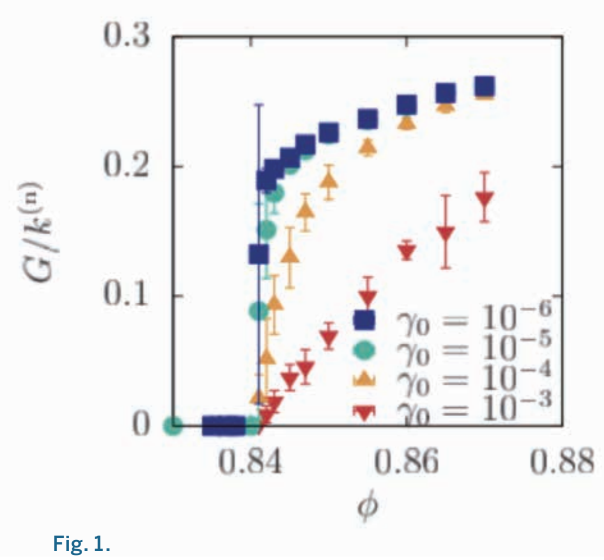

Fig. 1.
Shear modulus G versus packing fraction ϕ in frictional granular materials under different strains γ_0.

Introduction to Publicly Offered Research in Group C02

AE spectrum as an indicator of jamming on the fault plane

Ikuro SUMITA, Kanazawa Univ.

Slow earthquakes commonly accompany tremor. Can we deduce the degree of jamming on the fault plane using tremor ? An acoustic emission (AE) is excited when a granular material (e.g., fault gouge) is sheared. Here we conduct laboratory experiments focusing on the effect of particle diameter (d) on the AE spectrum (in collaboration with H. Fukumizu). Figure 1 shows the AE acceleration waveform, which is separated into three frequency bands. The two sensors are located at antipodal positions. The waveforms of the low- and middle-frequency bands that were recorded by the two sensors are out-of-phase and in-phase, respectively, and their frequencies decrease with container size, indicating that they originate from eigen oscillations. However, the high-frequency band is likely to originate from interparticle friction. Figure 2 shows the d-dependence of the spectra, where both the absolute and relative power of the high-frequency band increase with d. Broadband AE excitation resembles tremor and very-low-frequency earthquakes, suggesting that their spectra may be used to infer jamming on the fault plane.

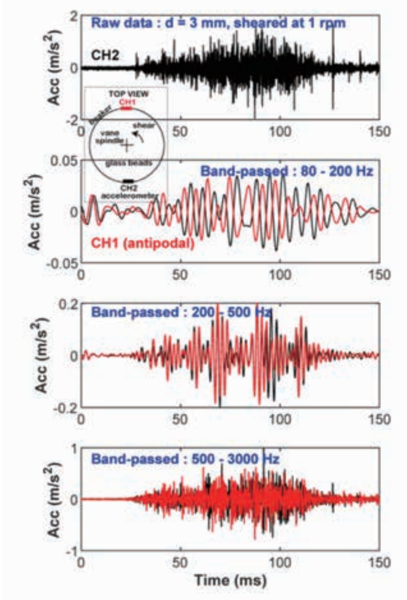

Fig. 1.
An example acceleration waveform (d = 3 mm). The red and black waveforms are those for the two AE sensors, which are located at antipodal positions on the sample (CH1 and CH2; inset).

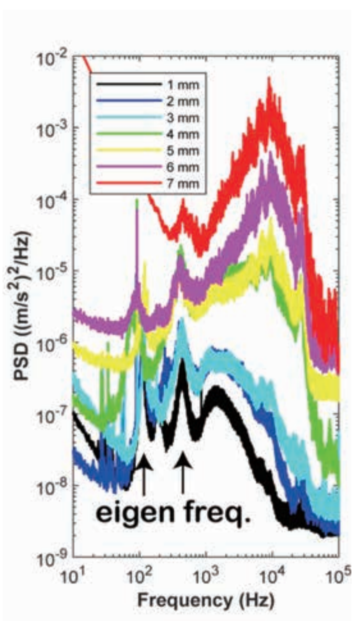

Fig. 2.
d-dependence of the acceleration spectrum (200-s long, shear rate = 1 rpm).

Introduction to Publicly Offered Research in Group C02

Theoretical and numerical study of slow and ordinary earthquakes and frictional phenomena

Hiroshi MATSUKAWA, Aoyama Gakuin Univ.

We derive the rate- and state-dependent friction law from a microscopic model of a single asperity. The frictional force vanishes at the low-velocity limit for the case where the direct term (A term) dominates. This is due to the fact that the thermal fluctuation assists the sliding motion, even when the magnitude of the driving force is small. The frictional force vanishes in the low-velocity limit because the actual contact area can not exceed the apparent contact area also for the case where the indirect term (B term) dominates. It is therefore expected that the vanishing frictional force can generally be observed at the low-velocity limit.

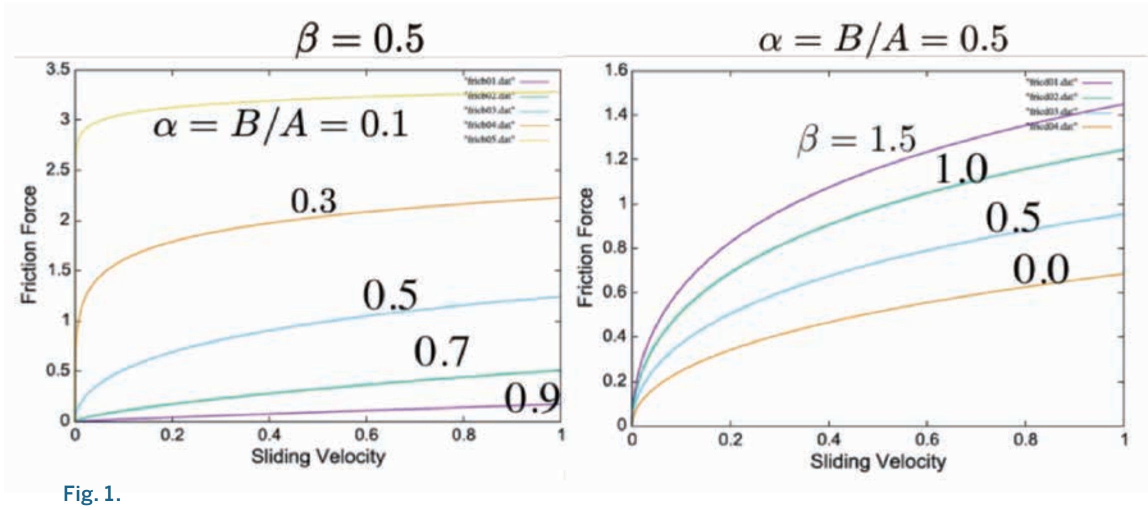

Fig. 1.
Sliding velocity dependence of the frictional force. β represents the power of the size distribution of the asperity.

Science of Slow Earthquakes
Activity report

Jul. 18, 2019
WS for early career researchers

Multidisciplinary workshop for early career researchers

Akiko TAKEO, ERI, UTokyo

We held a multidisciplinary workshop for early career researchers on July 18, 2019, at the University of Tokyo to obtain a better understanding of the ongoing research across the various academic fields investigating slow earthquake processes, including geophysics, geology, and physics. There were 25 participants, including Ph.D. students, and 12 early career researchers (completed Ph.D. within 10 years) gave presentations on their research fields. This workshop allowed us to share basic knowledge that was beneficial for the “International Joint Workshop on Slow Earthquakes 2019” that was held in September at Sendai. We also discussed heterogeneous structures around the plate interface and analogue experiments in physics.

Upcoming events for early career researchers will be planned by a range of organizers, and will include both research/academic and social events.

Photograph of the first presentation during the workshop.

Science of Slow Earthquakes
Activity report

Overseas research program

Satoru BABA, D1, ERI, UTokyo

Feb.21- Mar.22, 2019

I visited Institut de Physique du Globe de Paris (IPGP) in France, and worked with Dr. Jean-Pierre Vilotte, Dr. Natalia Poiata, and Dr. Mariano Supino on the development of a detection method for very low frequency earthquakes (VLFEs). Dr. Poiata developed a statistical detection and location method for low frequency earthquakes (LFEs); I attempted to apply this method to the detection of VLFEs, whose observed frequencies are lower than those of LFEs. I also had numerous seismological discussions, including on the spatiotemporal relationship between LFE and VLFE activity, with IPGP researchers. This opportunity was a rewarding experience for me.

So OZAWA, D1, UTokyo

Mar.04-29, 2019

I visited the Department of Geophysics at Stanford University from 4-29 March 2019. I worked with Associate Professor Eric Dunham on modeling the earthquake cycle on nonplanar faults, and developed a numerical simulation code that employed a joint finite difference and boundary integral approach. I also attended a number of geophysical seminars, and learned about the recent trends in earthquake science in the United States, such as injection-induced seismicity and machine learning. I also had the opportunity to get a feel for the research/academic atmosphere by talking to and interacting with students in the department.

Kodai SAGAE, D1, Tohoku Univ.

Jun.06-20, 2019

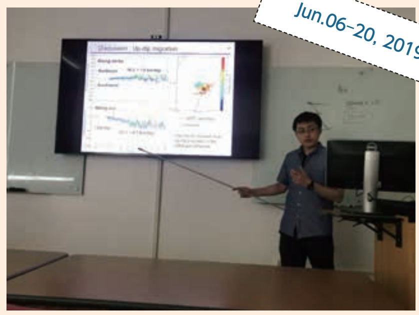

My research focus is on the detection and hypocenter determination of deep low-frequency tremors using a seismic array. I visited the University of California-Santa Barbara (UCSB), and learned about noise field characteristics from Professor Toshiro Tanimoto. We also had informative and insightful discussions on array analysis techniques and the accuracy of tremor detection by properly distinguishing tremors from noise. This experience provided me with a wealth of new seismological knowledge. It was also interesting to hear about the research UCSB students were undertaking, as well as discuss my own research. I enjoyed sightseeing in Santa Barbara and Solvang, California, on the weekends. I would like to thank the "Science of Slow Earthquakes" project for providing me with such a valuable opportunity.

Taihei FUKUDOME, M2, Kyushu Univ.

Aug.21-Sep.14, 2019

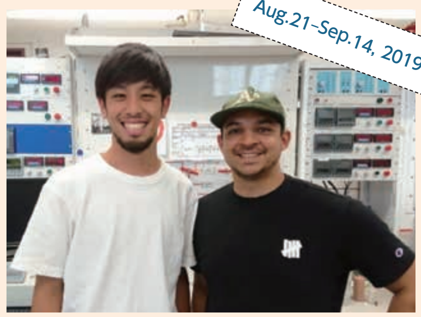

I visited the ETH Zürich and performed high-temperature impact experiments using acoustic emission (AE) sensors. I primarily observed the seismic waves from AE sensor signals, and calculated the seismic moment from these signals. I had the opportunity to discuss my research with Prof. Nicholas D. Spencer. He gave me helpful advice on the friction of polymer gels, which are used in our experiments, and we discussed universality beyond various materials and its relation to actual earthquake processes. This opportunity allowed me to conduct laboratory experiments and implement observational methods that I had not previously performed, such that I could compare this approach with our experimental method. This experience will help me to construct a more sophisticated experimental system.

Science of Slow Earthquakes
Activity report

Report on the cancelled workshop on slow and fast earthquakes in Chile

Satoshi IDE, EPS, UTokyo

Oct.28, 2019
The cancelled workshop in Chile

Chile extends more than 4000 km along the Pacific coast of South America, and the offshore Chilean subduction zone is a highly active plate boundary where the Nazca and Antarctic plates are subducting beneath the South American plate. Some of the world's largest earthquakes have occurred in Chile, and a number of slow earthquakes have occurred along the Chilean subduction zone, making this an extremely interesting region for both megathrust and slow earthquake studies. A combination of recent great earthquakes and economic development has aided in the improvement of the Chilean geodetic and seismic monitoring networks. The high degree of scientific interest in the seismic processes along the Chilean subduction zone makes Chile a perfect place to hold workshops for the JSPS KAKENHI Project, Science of Slow Earthquakes. Therefore, the second co-organized overseas workshop, "The 1st International Workshop on Slow and Fast Earthquakes", was scheduled to be held in Santiago, Chile, on October 28-30, 2019. Including about 30 Japanese researchers, about 100 international researchers have registered for the workshop.

However, Santiago began to enter a state of unrest about ten days before the workshop. What began as high school students free-riding the metro services in protest of recent fare increases quickly escalated into demonstrations, riots, arson, and looting, with a state of emergency declared and a curfew issued. This occurred about a week before many of the workshop participants were set to begin their travels to Chile. Although there were no travel bans or other restrictions from the embassy, the University of Chile was closed, which made it unlikely that the workshop venue would be available for the scheduled workshop dates. Therefore, the workshop was cancelled on October 22 to avoid the risk of continued unrest and venue unavailability.

Most of the Japanese participants stopped traveling at this point. Mr. Wang (UTokyo), who was already in Chile, returned to Japan after shortening his schedule since the university was closed and he was unable to study. Despite this situation, several Japanese researchers still chose to travel to Chile. Four from UTokyo, three from Kyoto Univ., and one from Kobe Univ. made the journey, even though the demonstrations, unrest, and general confusion continued. The contingent from UTokyo, including myself, visited Santiago and Valdivia, largely following the original workshop plan.

Fortunately, the state of emergency and curfew were lifted by the time I arrived in Santiago on October 27, and the city was regaining order. The demonstrations were mainly peaceful, and the hotels, supermarkets, and restaurants were all open, such that there were no inconveniences to life. In fact, we were very satisfied with the food and beverage. The subway services were unreliable and potentially unsafe due to the protests, but Uber was a very useful option that we used daily.

Group photograph

However, although it was generally calm, there were still ongoing demonstrations that occasionally escalated into violence. I got anxious when I heard news of arson while we were in Santiago, and I was surprised to smell tear gas flowing into the Uber car while driving around the city center.

The workshop was changed into a mini research meeting for those who traveled to Santiago. While less than 20 people attended the meeting, it provided the opportunity for each person to thoroughly discuss their research over the course of two days. We were also able to visit the control center at Centro Sismológico Nacional (CSN) and an observation station after the meeting. As an individual, I was able to exchange information and ideas with Chilean researchers, outline plans for future slow earthquake research possibilities in southern Chile, and obtain new data; I was ultimately satisfied with these achievements. I then visited Valdivia to look for traces of the Great Chilean Earthquake, which occurred about 60 years ago.

Unexpected things happen, even in Chile, which is considered one of the safest and most stable countries in South America. This highlights that international collaborations can sometimes be difficult. We have now returned to Japan, but Chile is still in a state of unrest. I am deeply grateful to the Chilean organizer, Sergio Ruiz, who welcomed our visit and was very accommodating, even though he was forced to make difficult decisions regarding the workshop itself. I hope that their daily life and research will soon return to normal.

Visit to CSN

Science of Slow Earthquakes

Newsletter04

Publisher/Contact

Office for Scientific Research on Innovative Areas:
Science of Slow Earthquakes
1-1-1 Yayoi, Bunkyo-ku, Tokyo, JAPAN 113-0032
(within the Earthquake Research Institute,The University of Tokyo)
TEL: +81-3-5841-2956
E-mail: sloweq-office@eri.u-tokyo.ac.jp

Date of issue 2020.Feb.

http://www.eri.u-tokyo.ac.jp/project/sloweq/en/